

FROM NEARBY LOW LUMINOSITY AGN TO HIGH REDSHIFT RADIO GALAXIES: SCIENCE INTERESTS WITH SKA

P. KHARB^{1,2}, D. V. LAL¹, V. SINGH³, J. BAGCHI⁴, C. H. ISHWARA CHANDRA¹, A. HOTA⁵, C. KONAR⁶, Y. WADADEKAR², P. SHASTRI², M. DAS², K. BALIYAN³, B. B. NATH⁷, M. PANDEY-POMMIER⁸

¹National Centre for Radio Astrophysics - Tata Institute of Fundamental Research, Post Bag 3, Ganeshkhind, Pune 411007, India

²Indian Institute of Astrophysics, II Block, Koramangala, Bangalore 560034, India

³Astronomy & Astrophysics Division, Physical Research Laboratory, Ahmedabad 380009, India

⁴Inter-University Centre for Astronomy and Astrophysics, Pune, India

⁵UM-DAE Centre for Excellence in Basic Sciences, Vidyanagari, Mumbai 400098, India

⁶Amity Institute of Applied Sciences, Amity University Uttar Pradesh, Sector 125, Noida 201303, India

⁷Raman Research Institute, C. V. Raman Avenue, Sadashivanagar, Bangalore 560080, India and

⁸Univ Lyon, Univ Lyon1, Ens de Lyon, CNRS, Centre de Recherche Astrophysique de Lyon UMR5574, 9 av Charles Andr, 69230, Saint-Genis-Laval, France

Draft version May 1, 2018

ABSTRACT

We present detailed science cases that a large fraction of the Indian AGN community is interested in pursuing with the upcoming Square Kilometre Array (SKA). These interests range from understanding low luminosity active galactic nuclei in the nearby Universe to powerful radio galaxies at high redshifts. Important unresolved science questions in AGN physics are discussed. Ongoing low-frequency surveys with the SKA pathfinder telescope GMRT, are highlighted.

Keywords: galaxies: active — galaxies: Seyfert — quasars: general — BL Lacertae objects: general — radio continuum: galaxies

1. INTRODUCTION

Active galactic nuclei (AGN) are the centres of galaxies that emit copious amounts of radiation spanning the entire electromagnetic spectrum. It is now widely believed that AGN are accreting supermassive black holes (SMBH; masses $10^6 - 10^9 M_{\odot}$), where the enormous energy is the outcome of the release of gravitational potential energy (Lynden-Bell 1969; Ho & Kormendy 2000). Somewhere in the interface between the SMBH and the accretion disk, bipolar jets or outflows are launched (e.g., Rees et al. 1982). The details of the launch mechanism are still unclear, although magnetic fields are widely believed to be instrumental in the production and collimation of these outflows (Blandford & Znajek 1977; McKinney 2006; Tchekhovskoy et al. 2011). Strong and prominent emission lines in the optical-infrared spectrum, which are considered to be the hallmark of AGN, are produced in fast-moving gas clouds around the black hole-accretion disk system (the “central engine”): different cloud speeds and electron densities have led to the demarcation into broad and narrow line regions (BLR, NLR). The BLR in some AGN are obscured from certain lines of sight by a dusty torus or a warped accretion disk, giving rise to the classification of type 1 (BLR and NLR visible) and type 2 (NLR visible but BLR obscured), and a unified scheme that attempts to link the two types on the basis of orientation (Antonucci 1993; Netzer 2015). Seyfert type 1s (with broad and narrow permitted emission lines in their spectra) and type 2s (with only narrow permitted and forbidden lines in their spectra) are expected to be the same phenomenon, differing only in orientation.

The development of radio interferometry in the 1960s led to the discovery of kiloparsec-scale jets in AGN. Large-scale jets that are observed in only about 15–20% of AGN, emit at radio frequencies via the synchrotron

process. Highly energetic electrons in these jets sometimes emit optical and X-ray synchrotron photons as well (Sparks et al. 2000; Worrall et al. 2001; Harris & Krawczynski 2006). It was first pointed out by Fanaroff & Riley (1974) that kiloparsec-scale jets in radio galaxies exhibited primarily two radio morphologies: the Fanaroff-Riley (FR) type I galaxies had broad jets that flared into diffuse radio plumes / lobes, while the FR type II galaxies had collimated jets that terminated in regions of high surface brightness called “hot spots” with the back-flowing plasma or the plasma left behind by the advancing jet, forming the radio lobes. The total radio power of the FRI and FRII sources also differed: the dividing line at 178 MHz was at $L_{178} \simeq 2 \times 10^{25} \text{ W Hz}^{-1}$, with the FRII sources being more radio powerful. The FR dichotomy is one of the major unresolved problems in jet astrophysics: it is not clear why the jets in FRIIs are powerful enough to produce hot spots, while they apparently lack power in FRIs. Differences in the mass or spin of the SMBH, accretion rate and/or mode, jet-medium interaction, host galaxy type and the galactic environments, are some of the explanations put forward to explain the FR dichotomy (Prestage & Peacock 1988; Baum et al. 1995; Meier 1999; Hardcastle et al. 2007).

The radio-loud unified scheme proposes that BL Lac objects are the pole-on counterparts of FRI radio galaxies while the radio-loud quasars are the pole-on counterparts of FRII radio galaxies (Urry & Padovani 1995). BL Lacs and quasars are collectively referred to as “blazars”. Rapid variability at all wavelengths, high degrees of polarisation and superluminal jet motion, which are all the defining characteristics of blazars, are fully consistent with the suggestion of relativistic jets pointing close to our line of sight. Spectral energy distributions (SEDs) generated from multiwavelength studies of these blazars have revealed interesting trends: the synchrotron emis-

sion peaks at submm to IR ($\nu \sim 10^{13} - 10^{14}$ Hz) for the low frequency-peaked BL Lacs (LBLs) and flat-spectrum radio quasars (FSRQs), while they peak at UV to X-rays ($\nu \sim 10^{17} - 10^{18}$ Hz) for the high frequency-peaked BL Lacs (HBLs) (Padovani & Giommi 1995). Sambruna et al. (1996); Fossati et al. (1998) and others have suggested that there are intrinsic differences in the physical parameters of these blazar sub-classes, with HBLs having higher magnetic fields/electron energies and smaller sizes than LBLs and FSRQs.

The vast majority of AGN however, do not exhibit powerful radio jets or outflows. Seyfert galaxies and LINERs¹ fall under this category. Kellermann et al. (1989) classified AGN into the “radio-loud” and “radio-quiet” categories on the basis of their ratio (R) of radio flux density at 5 GHz to optical flux density in the B -band: R was $\ll 10$ for radio-quiet AGN. Differences in black hole masses, spins, accretion rates/modes, have been proposed to explain the radio-loud/radio-quiet divide (Laor 2000; Tchekhovskoy et al. 2010; Sikora et al. 2007; Garofalo 2013; Lal & Ho 2010). According to the “spin paradigm”, powerful radio jets originate near rapidly spinning accreting SMBH found in bulge-dominated systems, and are launched at relativistic speeds via the magnetohydrodynamic (MHD) Blandford-Znajek (BZ) mechanism (Blandford & Znajek 1977). Alternatively, in the Blandford-Payne (BP) mechanism (Blandford & Payne 1982), jet power is extracted from the rotation of the accretion disk itself, via the magnetic field threading it, without invoking a rapidly spinning black hole. However, in both the processes the intensity and geometry of the magnetic field near the black hole horizon strongly influences the Poynting flux of the emergent jet (Beckwith et al. 2008). This has given rise to the “magnetic flux paradigm”, which proposes that jet launching and collimation require strong magnetic flux anchored to an ion-supported torus of optically thin, geometrically thick, extremely hot gas with poor radiative efficiency (Sikora & Begelman 2013). In general, a radiatively efficient fast accretion mode (or “quasar” mode) has typically been associated with a large fraction of “radio-loud” AGN, while a radiatively inefficient slow accretion mode (or “radio” mode) has typically been associated with “radio-quiet” AGN (Croton et al. 2006; Best & Heckman 2012).

There is also evidence to suggest that galaxy mergers influence the radio-loudness of sources (Heckman et al. 1986; Deane et al. 2014). We know that galaxy mergers are an important phase of galaxy evolution (Schweizer 1982; Mihos & Hernquist 1996; Cox et al. 2006). Mergers are especially important at high redshifts, where the galaxy density was higher compared to the present Universe. As all massive galaxies are expected to harbour SMBH in their centres (Kormendy & Ho 2013), galaxy mergers are expected to lead to a large fraction of binary black hole systems. Such systems have so far, however, been identified in only a handful of sources (e.g., Deane et al. 2014; Müller-Sánchez et al. 2015). Radio sources that exhibit double peaks in their emission line spectra are good candidates for binary AGN (Liu et al. 2010; Rosario et al. 2011; Comerford et al. 2013). As are sources exhibiting highly distorted jets and lobes, called X-shaped sources (Cheung 2007; Lal & Rao 2005, 2007).

Galaxy mergers are likely to be driving gas into the centres of merging galaxies, thereby providing fuel to be accreted on to the black holes. Yet not all dual AGN candidates exhibit one or two sets of bipolar kiloparsec-scale jets. The reasons for this absence are important but unclear. The search for dual AGN and a multi-wavelength study of dual AGN candidates can provide a different but unique perspective on the close interplay between the central SMBH and its host galaxy.

One way to detect dual AGN is through the technique of very long baseline interferometry (VLBI). For VLBI, unconnected radio telescopes located in separate parts of the world, work together to produce a single large radio telescope with milliarcsecond resolution. This translates to parsec-scales at the distance of the AGN we aim to study. One of the most robust detections of a binary black hole system have been made by Rodriguez et al. (2006) using multi-frequency VLBI. Moreover, multi-epoch VLBI observations are now determining jets speeds in blazars, radio galaxies, Seyferts and LINERs (e.g., Ulvestad et al. 1999; Lister et al. 2009). These studies have found that the jets in radio-loud AGN are typically faster than those in radio-quiet AGN. The reasons for the differences are not clear. Are jets being launched with different speeds by different mechanisms or are they getting slowed down by interacting with the surrounding medium? (e.g., Bicknell 1986; Laing & Bridle 2002). The role played by jet-medium interaction in jet propagation is another important unsettled question in jet astrophysics. Bent radio jets in radio galaxies residing in galaxy clusters demonstrate the significance of jet-medium interaction (e.g., O’Dea & Owen 1985; Lal et al. 2013), while VLBI observations suggest that jet differences occur close to the jet launching sites (e.g., Lister et al. 2009; Kharb et al. 2010).

High redshift radio galaxies (HzRGs) are known to reside in dense environments, and therefore, can be used as the tracers of (proto)clusters (Venemans et al. 2007; Galametz et al. 2012), as well as test cases for the study of jet-medium interaction. Since supermassive blackholes are essential ingredients of radio powerful AGN, the formation of SMBH at early epochs in the lifetime of the Universe, can also be probed with HzRGs. The host galaxies of HzRGs are among the most massive intensely star-forming galaxies and are believed to be progenitors of massive elliptical galaxies in the local Universe (McLure et al. 2004; Seymour et al. 2007). The radio luminosity function of HzRGs beyond redshift of 3 is poorly constrained. In fact, it is unclear whether there is a genuine dearth of HzRGs at $z > 3$ or the observed deficiency is merely due to selection effects. HzRGs are also complementary to the emerging population of Lyman break galaxies at high redshifts, which are less massive by one to two orders of magnitude compared to the host galaxies of HzRGs. Therefore, the identification and study of HzRGs is important to understand the formation and evolution of galaxies at higher redshifts and in dense environments.

Over the last two decades, supermassive black hole scaling relationships have become very well-established for both dormant and accreting SMBH. A clear corollary is strong coupling between the accretion processes that lead to a SMBH forming an AGN on the one hand, and star formation in their host galaxies on the other. When

¹ Low-Ionization Nuclear Emission-line Region

Table 1
SKA bands, including proposed changes in the low-frequency band definitions for SKA1-MID (Ref. ECP150027).

		MeerKAT	SKA-Now	SKA-Final
		ν (MHz)	ν (MHz)	ν (MHz)
SKA1-LOW		...	50-350	...
SKA1-MID	Band 1	580-1015	350-1050	475-875
	Band 2	900-1670	950-1760	795-1470
	Band 3	...	1650-3050	1650-3050

these accreting SMBH produce jets of plasma that reach hundreds of kpc, there is clearly feedback into the intra-cluster medium as well. AGN are thus key players in our cosmic history, but our physical understanding of the jet launch and feedback, has remained sketchy. SKA will be able to sample like never before the parameter space of not only luminosity, redshift, jet collimation, quenching, time-domain behaviour and the black hole mass ladder, but also of the life-span of AGN activity. In the sections ahead, we discuss the work that has been carried out in different science areas by a large fraction of the AGN community in India. Sections are divided around the key unresolved science questions in AGN physics. We describe how SKA will help in resolving these science questions. Details of upcoming SKA surveys and expected sensitivity levels are presented in Tables 1 and 2.

In this article, we have adopted the spectral index convention, $S_\nu \propto \nu^{-\alpha}$, where S_ν is the flux density at frequency ν and α is the spectral index.

2. JET FORMATION IN AGN

Comparing and contrasting sources that possess jets with those that do not, is crucial for learning about jet formation. We discuss below how the “radio-loud/radio-quiet” divide can be, and is being tested on different fronts. First, sensitive radio observations are detecting kiloparsec-scale radio structures (KSRs) in Seyfert and LINER galaxies. These jets and lobes can extend from a kiloparsec to 10 kpc, or more. The host galaxies of these are typically lenticular or S0-type. Second, sensitive radio observations are detecting giant radio jets in spiral galaxies. Both these findings are challenging the previous well-accepted suggestions in the literature that large radio jets are only produced in elliptical galaxies, and not in spiral galaxies (McLure et al. 1999). In the next two sections, we discuss these points individually.

2.1. KSRs in “Radio-quiet” Seyferts & LINERs

Gallimore et al. (2006) have detected KSRs in > 44% of Seyfert galaxies belonging to the volume-limited CfA+12 μ m sample when observed with the sensitive D-array configuration of the VLA at 5 GHz. Singh et al. (2015b) found that > 43% of Seyferts belonging to a sample derived from the VLA FIRST² and NVSS³ surveys, possessed KSRs. Low frequency observations with the GMRT at 610 MHz are finding an even larger fraction of KSRs in Seyfert and LINER galaxies (> 50%, Kharb et

al., in preparation).

While Seyfert galaxies have traditionally been categorised as “radio-quiet” AGN, Ho & Peng (2001) have demonstrated that when the optical nuclear luminosities are extracted through high resolution observations (e.g., from the *Hubble Space Telescope*) and the galactic bulge emission is properly accounted for by using specialized software like GALFIT, then the majority of Seyfert galaxies shift into the “radio-loud” class. Kharb et al. (2014) have confirmed this trend in the Extended 12 μ m Seyfert sample. Moreover, they found a continuous distribution in the radio-loudness parameters of Seyfert galaxies and low-luminosity FRI radio galaxies. From their FIRST+NVSS VLA study, Singh et al. (2015b) have found that $\sim 15\%$ of their Seyfert/LINER sample fall under the “radio-loud” category, following the definition of Kellermann et al. (1989).

We need to look closely at Seyferts with KSRs and low luminosity FRI radio galaxies with weak radio jets, which together constitute the low-luminosity “intermediate” AGN population. If accurate black hole masses can be estimated for all low-luminosity “intermediate” AGN, along with their core X-ray and radio luminosities, then they could be placed on the fundamental plane (e.g., Merloni et al. 2003), to see where they lie. If their fundamental plane is offset from the rest of the classical objects, it may suggest a new mode of disk-jet coupling in these sources.

To produce statistically robust results, studies like these are most efficiently carried out using large galaxy samples drawn from large area radio surveys. The SKA1-MID array has the potential to study weak KSRs in Seyfert, LINERs and low-luminosity FRI radio galaxies. The angular resolution that will be achieved ranges between 0.4'' at 1.4 GHz (band 2) and 0.07'' at 8.3 GHz (band 5). The three-tier survey at bands 1 and 2 (1 and 1.4 GHz) will also be ideal for carrying out this study (see Table 1 in Prandoni & Seymour 2015). It is expected that SKA will detect a much larger number of radio-“intermediate” sources, that will fill the radio-loud/radio-quiet gap.

2.2. Giant Radio Jets in Spiral Galaxies

With the advent of sensitive low radio frequency telescopes like the GMRT and LOFAR, several giant radio jets (extents $\gg 100$ kpc) that are hosted in massive spiral galaxies, have been discovered (e.g., Ledlow et al. 1998; Hota et al. 2011; Bagchi et al. 2014; Mao et al. 2015; Singh et al. 2015a). The standard paradigm to explain

Table 2
Expected Sensitivity Levels of SKA bands.

		Bandwidth	Field of View	<i>rms</i> noise
		(MHz)	(deg ²)	(μ Jy beam ⁻¹)
SKA1-LOW		250	39	$\sim 20^\dagger$
SKA1-MID	Band 1	700	1.4	~ 1.7
	Band 2	810	0.35	~ 0.8
	Band 3	1400	0.12	~ 0.7

Note: The listed sensitivity levels are achievable in one hour of integration time. \dagger SKA1-LOW is limited by confusion noise. To circumvent this, one can use frequencies ≥ 200 MHz and eventually reach *rms* noise levels of $\sim 10 \mu$ Jy beam⁻¹.

² Faint Images of the Radio Sky at Twenty cm (Becker et al. 1995)

³ NRAO VLA Sky Survey (Condon et al. 1998)

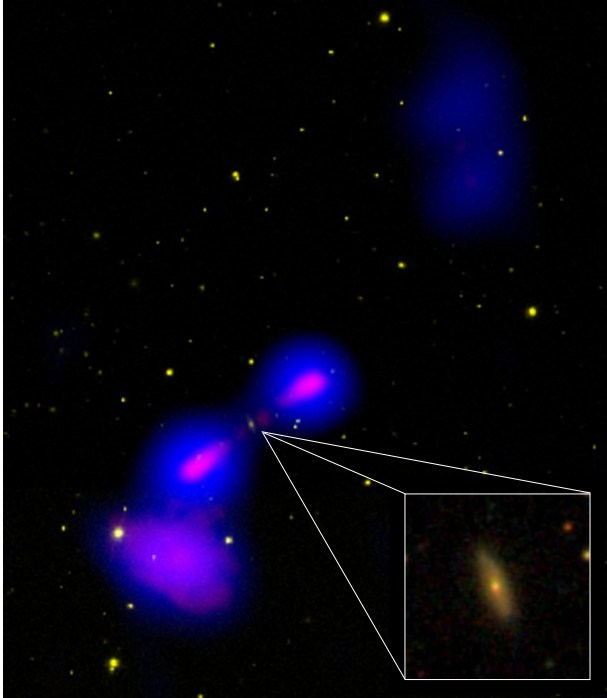


Figure 1. The composite image of Spica (Hota et al. 2011). The NVSS 1.4 GHz emission is in blue, while the GMRT 325 MHz emission is in red. The radio emission is superimposed on the optical image from SDSS. Inset shows the SDSS image of the host galaxy.

the elliptical hosts of large radio galaxies, invokes the process of two large spiral galaxies merging into an elliptical (e.g., Schweizer 1986; Barnes & Hernquist 1992). In this process, the central supermassive black holes of each spiral galaxy also merge and grow in mass. Therefore, the discovery of a few spiral galaxies hosting large or giant radio galaxies suggest alternate ways (other than mergers) of creating conducive physical conditions for the formation of radio galaxies. If the central black hole can grow big and spin fast, under whatever circumstances, it may be possible to create large radio jets.

The first large radio galaxy hosted in a disk galaxy (J0315–1906) was found by Ledlow et al. (1998). Hota et al. (2011) reported the finding of the second such galaxy ‘Spica’ (SDSS J140948.85–030232.5; see Figure 1), using SDSS⁴, NVSS and GMRT data. Recently, Bagchi et al. (2014) reported the case of a spiral host in the source J2345–0449 (see Figure 2). With the help of web-based citizen-scientists project (Radio Galaxy Zoo), Mao et al. (2015) detected another such galaxy, J1649+2635, from an initial sample of 65,492 galaxies. Using similar automated archive cross-matching of SDSS, NVSS and FIRST data, Singh et al. (2015a) have reported three new cases of spiral-host radio galaxies (viz., J0836+0532, J1159+5820, J1352+3126). Although J1649+2635 shows an optically blue grand-design spiral pattern, it is buried inside a huge old-stellar halo, unlike any spiral galaxy we know. Both J1352+3126 and J1159+5820 show clear signs of tidal interaction or past merger. So far, J0315–1906, Spica, J2345–0449 and

J0836+0532 are the only four clear cases of large radio galaxies hosted by spirals.

Out of these four galaxies, two of them are giant and show episodic activity: J2345–0449 is a double-double radio galaxy of extent 1.6 Mpc, and Spica is likely a triple-double radio galaxy of extent 1.3 Mpc. J2345–0449 is a massive spiral galaxy ($M_{\text{dyn}} \sim 1.0 \times 10^{12} M_{\odot}$), with a diameter of nearly 50 kpc, a fast rotation speed ($\sim 430 \text{ km s}^{-1}$) and a high central velocity dispersion ($\sigma \sim 300 \text{ km s}^{-1}$; Bagchi et al. 2014). Similarly, observations with the Subaru telescope have shown that Spica is large ($\sim 60 \text{ kpc}$) and has a rotation speed of $\sim 370 \text{ km s}^{-1}$ (Hota et al. 2014). Both these giant radio jets are therefore hosted by large and massive spiral galaxies.

Such galaxies have likely grown in isolation without mergers but with co-planar accretion directly from cosmic-filaments or surrounding medium. They are expected to be more numerous at higher redshifts. None of these sources have so far shown an FRI-type radio morphology. This is likely to be due to the lack of sensitivity, especially for the high redshift sources. Once we have a larger number of such sources, the following questions can be answered: is there a difference in the bar fraction or metallicity in these host galaxies, or the presence of double nuclei? Are there differences in the molecular gas fraction compared to other spiral galaxies? Observing large samples of massive spirals with the SKA (see Section 5.1 for more details), specifically at low radio frequencies, will increase the probability of finding several more spiral-host large radio galaxies, which have been missed in current surveys. Even before the operation of SKA1, the sample of such spiral galaxies will increase by two orders of magnitude due to optical spectroscopic surveys like DESI⁵. High-resolution VLBI imaging and polarisation mapping of the inner radio jets near the core, in the disk/corona collimation region, would be very informative for understanding the jet launching process in

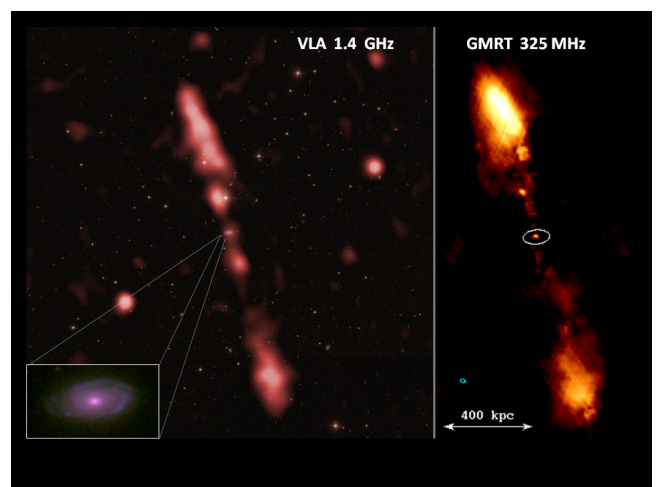


Figure 2. The composite image of J2345–0449 (Bagchi et al. 2014). The radio image from the NVSS at 1.4 GHz and the GMRT at 325 MHz are shown in red and orange. The inset shows the RGB-colour image of the host galaxy from CFHT.

⁴ Sloan Digital Sky Survey (York et al. 2000)

⁵ Dark Energy Spectroscopic Instrument

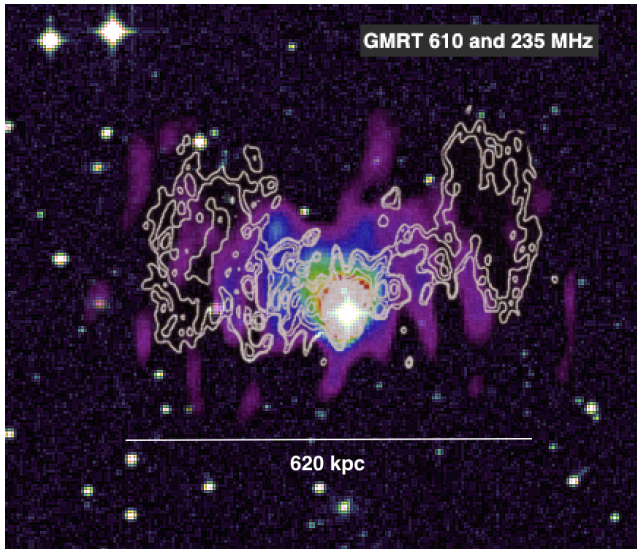


Figure 3. Sensitive GMRT observations at 235 and 610 MHz (in colour and contours) reveal a ~ 600 kpc-scale radio jet in the erstwhile core-dominated BL Lac object PKS 2155–304 (Pandey-Pommier et al. 2016).

these highly unusual AGN.

Using the VLA FIRST survey, Proctor (2011) and Machalski et al. (2001) have listed three dozen FRII or FRI/II sources with angular sizes between brightest regions $\gtrsim 3'$ and a flux density limit, from a 3000 deg^2 region. Extrapolating from these detections, and using Figure 1 from Johnston-Hollitt et al. (2015), we expect the SKA surveys to detect about a few times 10^4 giant radio galaxies (see also Kale et al. 2016 in these proceedings). If we make a conservative estimate that $\sim 10\%$ of these are in spiral hosts, we will observe a thousand new giant radio galaxies hosted by spirals. An all-sky radio continuum survey using SKA1 will provide statistically large samples so that we can finally study them as a distinct class of AGN.

3. JET MORPHOLOGY: CLUES TO FORMATION AND PROPAGATION

Jets in AGN span parsec to mega-parsec scales, and have speeds ranging from a few thousand km s^{-1} to a fraction of the speed of light. Their morphologies are diverse: they can be bent, S- or Z-shaped, flaring or highly collimated. They can possess terminal hotspots or be plume-like with no clear jet termination. These morphologies can indicate differences in the jet launch speeds and/or jet-medium interaction. Attempts to unify this large variety of jet structures have been made. We discuss ahead the successes and failures of these attempts.

3.1. The FR Divide & Radio-loud Unification

The simple radio-loud unified scheme linking BL Lac objects to FRI and quasars to FRII sources, has been challenged by Kharb et al. (2010) on the basis of their kiloparsec-scale radio study of the MOJAVE⁶ blazar sample. Kharb et al. examined the MOJAVE sample of 135 blazars (Lister et al. 2009), using high-resolution 1.4 GHz data from the VLA, and found that a substantial fraction ($\approx 20\%$) of MOJAVE quasars and BL Lacs

⁶ Monitoring of Jets in AGN with VLBA Experiments. <https://www.physics.purdue.edu/MOJAVE>

had total radio powers that were “intermediate” between FRIs and FRIIs (see Figure 4). Many BL Lac objects had lobe luminosities ($\approx 30\%$) and hot spots ($\approx 60\%$) like quasars. In addition, they found a strong correlation between the kiloparsec-scale lobe luminosities and parsec-scale jet speeds: the large-scale jet and lobe knew about the small-scale jet as it was launched. It therefore appeared that the fate of the AGN was decided at its birth!

These results have important implications for the inner workings of AGN. Therefore, they need to be re-examined with higher sensitivity radio data, as will become available with SKA. For instance, Figure 3 shows an example of an FRI BL Lac object which was earlier known to host a highly variable compact radio core, but reveals extensive diffuse emission in a jet extending to 620 kpc, in a deep GMRT study at 235 and 610 MHz (Pandey-Pommier et al. 2016). Could some BL Lac objects shift into the FRII luminosity category (contrary to the expectations of the Unified Scheme) with the detection of diffuse lobe emission? As is clear from Figure 4, the much lower sensitivity limit of SKA1-MID at GHz frequencies, is likely to detect nearly twice as many “intermediate” or hybrid FRI/II sources (e.g., Lal et al. 2010; Stanley et al. 2015), than previous studies carried out with the VLA. Our (historical) VLA observations at 1.4 GHz could not detect extended radio emission below $\sim 10\text{--}50 \mu\text{Jy beam}^{-1}$, but SKA1-MID will be able to detect emission that is as low at $0.7 \mu\text{Jy beam}^{-1}$ (Table 1; Dewdney et al. 2013), thereby increasing the overall sensitivity by a factor of 10 to 70.

These sensitive data will become available for a much larger population of radio sources including the so-called “core-only” sources ($\approx 7\%$ in the MOJAVE complete sample; Kharb et al. 2010, see upper limits in Figure 4). There are suggestions that these “core-only” blazars are another beast altogether (e.g., Punsly et al. 2015). SKA will find out whether this is a new class of sources or sources with very faint extended emission beyond the reach of present day radio telescopes. Perhaps they exhibit episodic activity and are currently switched off: the faint emission from the previous episodes is not detectable.

The SKA1-LOW and SKA1-survey⁷ are ideal for detecting the full extent of the diffuse lobe emission in radio galaxies and blazars. SKA1-LOW is expected to operate between 0.05–0.35 GHz, while the SKA1-survey will operate between 0.65–1.67 GHz (Table 1; Dewdney et al. 2013). The resolution of SKA1-LOW would typically be around 11 arcsec, while the SKA1-survey will be around 0.9 arcsec. The three-tier survey at bands 1 and 2 (1.0 and 1.4 GHz) will be ideal for carrying out this project (Prandoni & Seymour 2015).

3.2. Probing Blazar Nuclei with SED Modelling

A large number of blazars (radio-loud quasars and BL Lac objects) are being detected in the *Fermi* gamma-ray survey of the sky. For many sources, it is difficult to find their association in various energy regimes and

⁷ We note that SKA1-survey in Australia has been deferred in the SKA1 re-baselining of March 2015; see <https://www.skatelescope.org/wp-content/uploads/2014/03/SKA-RBS-outcome.pdf>

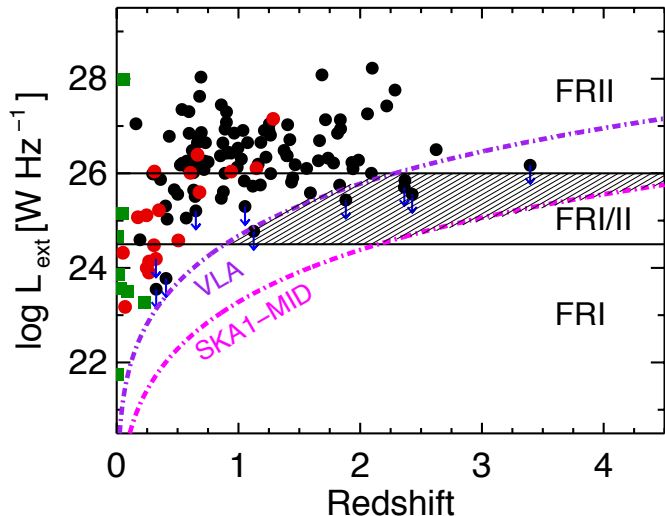


Figure 4. 1.4 GHz extended luminosity versus redshift for the MOJAVE sample (Kharb et al. 2010). Black and red circles denote quasars and BL Lac objects, respectively, while green squares denote radio galaxies. Core-only sources are represented as upper limits with downward arrows. The solid lines indicate the FRI–FRII divide (extrapolated from 178 MHz to 1.4 GHz assuming a spectral index, $\alpha=0.8$), following Ledlow & Owen (1996) and Landt et al. (2006). The purple line denotes the sensitivity limit for the historical VLA which was used to carry out the MOJAVE study, while the magenta line denotes the sensitivity limit for the upcoming SKA1-MID array (see Table 1; Dewdney et al. 2013). SKA will be able to detect nearly twice as many “intermediate” or “hybrid FRI/II” sources, compared to previous studies.

their identification (e.g., LBL, HBL) due to lack of extensive data. Multi-frequency observations at all frequencies along with optical and radio polarization measurements are required: while one can use polarization information to identify and broadly classify blazar classes, continuum fluxes at all possible energy regimes are required to generate the SEDs. For instance, the blazar candidate CGRaBS J0211+1051 was detected by *Fermi* in a flaring mode. Chandra et al. (2012) carried out optical polarization observations of this source with the Mount Abu Infrared Observatory, India, in 2011, and detected high and variable degree of polarization (9–20%). They therefore proposed the source to belong to the LBL class. To confirm this, a multi-frequency study was carried out for this source using data from the MOJAVE, *Planck*, *WISE*, *Swift*, Mount Abu Observatory, *Fermi* and *VERITAS*. The SED showed that low energy (synchrotron) peak fell at 10^{14} Hz, confirming it to be a low-energy peaked blazar. The light-curves showed variations in the high energy gamma-rays to be correlated with X-ray, UV and optical variations, indicating their co-spatial origin (Chandra et al. 2014). Multi-band continuum data from SKA will greatly benefit generation of SEDs for blazars while VLBI data will be useful for localising the emission regions in jets. Classifying a greater number of blazars into various sub-categories can help us isolate the essential emission or physical mechanisms that are in play in these sources.

3.3. Estimating Radio Lobe Energetics

X-ray observations of radio galaxy lobes have shown that the electrons responsible for the synchrotron radi-

ation in radio wavelengths can also scatter the cosmic microwave background (CMB) radiation photons to X-ray wavelengths. Tamhane et al. (2015) discovered inverse Compton scattering by electrons in the lobes of a high redshift giant radio galaxy. CMB up-scattering is easier to detect at higher redshifts. This up-scattering requires that the Lorentz factors of the electrons be of order $\sim 10^4$, which implies that the regions in the lobe which would be X-ray bright would also be bright at low radio frequencies (few hundred MHz), for typical values of magnetic fields (Nath 2010). However, the surface brightness of these regions is likely to be low. Observations with SKA would be useful in determining the physical processes at work in the radio lobes (back flow, cooling of electrons due to adiabatic expansion of lobe, through radiation etc.).

4. JET KINEMATICS AND MAGNETIC FIELD STRUCTURE

Differences in jet launching speeds and magnetic field structures are widely believed to be important in explaining the wide variety of jets observed in AGN. Multi-epoch VLBI observations are essential to measure jets speeds on parsec and sub-parsec scales. We discuss multi-epoch VLBI below in Section 4.1. The feasibility of carrying out VLBI and polarization-sensitive VLBI with SKA (or SKA-VLBI) has been discussed by Paragi et al. (2015). Polarization-sensitive VLBI (VLBP) observations can estimate the projected magnetic field structures in parsec-scale jets (Gabuzda et al. 1994). Polarisation measurements in kiloparsec-scale jets and lobes can reveal the effects of jet-medium interaction on inter-galactic scales (Liu & Pooley 1991; Laing 1996; Kharb et al. 2012).

4.1. Jet Speeds from Multi-epoch VLBI

Using VLBI images of a rigorously selected sample of Seyfert galaxies, Lal et al. (2004) have shown that the radio properties of the compact parsec-scale features are consistent with the unified scheme for Seyfert galaxies (see Section 1), with no significant evidence for relativistic beaming in their jets (see also Lal et al. 2011). Some parsec-scale features in these sources could be termination points of radio jets. The high-resolution, parsec-scale study of low-luminosity AGN is challenging because these sources have very low radio flux densities, typically less than a few milli-Jansky. Therefore the correlated flux densities of only a handful of sources meet the sensitivity thresholds currently offered by global VLBI, which can currently only study AGN with flux densities of least a few milli-Jansky. SKA-VLBI will be able to decrease this flux density limit by several orders of magnitude. This will allow us to study jets and jet speeds in low luminosity AGN, just as they are launched from the black hole - accretion disk systems.

4.2. Magnetic Fields on Parsec-scales

VLBP observations of FRI radio galaxies at 8 GHz with a global VLBI array by Kharb et al. (2005) were among the first observations carried out on this relatively weak class of sources. Almost all previous such observations had been carried out on the more radio powerful FRII radio galaxies and blazars. Kharb et al. (2005) found a 100% detection rate of jet polarization in the four FRI radio galaxies they observed and a suggestion

of a “spine-sheath” magnetic field structure. Furthermore, the detection of significant core polarization was consistent with FRI radio galaxies lacking the putative dusty torus, the inner ionized region of which should have depolarized the core emission. The global VLBI array used in this study included the 100 m Effelsberg antenna: without the inclusion of this large single dish telescope, the VLBI array would not have been as sensitive and the success rate of detection would not have been 100%. A multi-frequency (5, 8, 15 GHz) VLBP study of these sources revealed a gradient in rotation measure (RM) across the jet of the FRI galaxy, 3C 78. Such a gradient suggests the presence of a helical magnetic field (Blandford 1993; Kharb et al. 2009; Hovatta et al. 2012; Gabuzda et al. 2014). Similar multi-frequency VLBP observations of a complete sample of UGC FRI radio galaxies, revealed sheath-like magnetic field structures in several sources, which are also consistent with helical magnetic fields (Kharb et al. 2012) (see also Laing (1993); Reichstein & Gabuzda (2010)).

SKA-VLBI with SKA1-MID and/or SKA1-SUR, observing together in the 1 – 15 GHz frequency range with the current VLBI arrays and future large aperture telescope like FAST (Nan et al. 2011), is expected to outperform current global VLBI arrays including even the most sensitive current telescopes (Paragi et al. 2015). Faraday rotation measurements and the search for RM gradients in both the approaching and receding jets of relatively-plane-of-sky radio galaxies of the FRI and FRII types, need to be carried out, in order to probe the complex magnetic field structures in jets, without relativistic effects that can dominate in the low inclination blazars. Since radio galaxies are much weaker than blazars in total radio emission, this study can only be carried out for a large enough number of sources with the future SKA-VLBI.

4.3. Magnetic Fields on Kiloparsec-scales

Multi-frequency polarization-sensitive observations with the VLA of a sample of 13 FRII radio galaxies, revealed interesting correlations on kiloparsec-scales (Kharb et al. 2008). A strong correlation between lobe depolarization and lobe spectral index (“Liu-Pooley effect”) was observed: radio lobes with a flatter spectrum exhibited lower depolarization. The lobe depolarization difference was correlated with the arm-length ratio: the shorter lobe in the source was more depolarized (see also Pedelty et al. 1989; Laing 1996). This strongly suggested that lobe depolarization depends significantly on environmental asymmetries in radio galaxies. Most interestingly, Gabuzda et al. (2015) have recently found suggestions for an ordered toroidal magnetic field component in the AGN 5C 4.114 on kiloparsec scales, through RM observations. Arcsecond-scale polarimetric observations can therefore provide important clues about the kiloparsec-scale environments of radio galaxies and blazars, as well as infer the presence of large-scale magnetic fields in their jets and outflows. SKA will detect fainter polarization signals on smaller spatial scales in the cores, jets, lobes and hotspots of radio galaxies, than is feasible with the current radio telescopes. This will be crucial in detecting signatures of ordered magnetic fields on a range of spatial scales in radio galaxies, or examining the intervening medium be-

tween the galaxies and us in much finer detail, with RM data.

5. AGN LIFETIMES AND DUTY-CYCLE

The lifetimes of radio sources have been inferred from several arguments. Spectral ageing analysis has been a powerful tool to infer radio source ages. Giant radio galaxies (GRGs) push the limits of the lifetimes for radio sources. It is also clear that AGN activity is episodic in nature (e.g., Davies 1990; Saikia & Jamrozy 2009). Attempts have been made to infer the AGN duty-cycle (e.g., Greene & Ho 2007). These are essential to understand why only a fraction of all galaxies in the Universe have nuclei that are “active”, even though all massive galaxies host supermassive black holes.

There have been attempts to investigate the lifetime and duty-cycle of AGN activity by studying radio galaxies exhibiting two pairs of lobes that are formed during two different phases of AGN activity (e.g. Jamrozy et al. 2009; Konar et al. 2013a). It is important to note that despite the availability of thousands of radio galaxies in various radio surveys, only a few dozen are confirmed ‘double-double radio galaxies’ (DDRGs; Schoenmakers et al. 2000; Nandi & Saikia 2012). The paucity of DDRGs can be understood as a lack of radio data with optimum sensitivity and resolution to detect radio structures of different spatial scales and surface brightness. Using deep 610 MHz GMRT observations, Singh et al. (2016) recently reported the discovery of a ‘triple-double radio galaxy’ (TDRG) J1216+0709, which exhibits three pairs of lobes from three different AGN activity episodes. The different structures seen in the GMRT image are undetected in all the previous radio surveys (e.g., FIRST, NVSS, VLSS, TGSS) due to the lack of optimum sensitivity and resolution. Therefore, more sensitive multi-frequency, multi-resolution observations from SKA are expected to detect radio structures from episodic AGN activity, that have so far remained undetected.

5.1. Giant Radio Galaxies

GRGs can be used as pointers of black hole physics and ‘barometers’ of the intergalactic medium in the cosmic web (e.g., Nath 1995; Malarecki et al. 2013). GRGs, whose lobes span ~ 1 Mpc or more are among the largest, most luminous objects in the Universe (Ishwara-Chandra & Saikia 1999). Due to sensitivity limitations of the present day radio telescopes, most of the GRGs found so far are in the nearby universe ($z \lesssim 0.7$). Recently, Sebastian et al. (2015, in preparation) have discovered a 2.2 Mpc giant radio source at a redshift of 0.56 in the field of LBDS-Lynx⁸. This appeared as a faint elongated source in the deep 150 MHz images with the GMRT, implying that the deeper radio surveys at low frequencies such as SKA-LOW have the potential to discover many giant radio sources at redshift > 0.5 .

It is unclear if the large sizes of GRGs reflect the high efficiency of radio jets produced from the central engine, or they grow to enormous sizes due to their favourable location within a low density ambient medium. Approximately half of the baryons in the present day Universe are still unaccounted for (‘missing’), in the sense that these baryons are believed to reside in the large galaxy

⁸ Leiden-Berkeley Deep Survey - Lynx

filaments, in the form of warm-hot intergalactic medium (WHIM), as part of the cosmic-web structure of the universe (Davé et al. 2001; Werner et al. 2008). The large extents of GRGs provide an excellent opportunity to use them as barometers for probing the physical properties of this WHIM gas (its temperature, pressure and magnetic field). For this purpose a sensitive search using SKA and LOFAR for Mpc scale radio sources in the vicinity of galaxy filaments and perhaps inside the voids, surrounded by sheets of galaxies would be extremely valuable. The discovery of large numbers of giant radio galaxies in the distant universe will be greatly facilitated by the concurrent operation of SKA1 and LSST⁹. Accurate photometric redshifts for millions of galaxies provided by LSST will be critical in this effort.

In Section 2.2, we had estimated the number of GRGs likely to be detected with SKA surveys by extrapolating from the detections seen in VLA FIRST survey images (Proctor 2011; Machalski et al. 2001) and Figure 1 from Johnston-Hollitt et al. (2015). To recapitulate, an all-sky radio continuum survey using SKA1 will provide statistically large samples of a few times 10^4 GRGs.

5.2. Double-double Radio Galaxies

DDRGs exhibit two episodes of jet activity, where a new pair of jets plows through the cocoon material dumped by previous jet activity. The duration of the active phase is a few to a few 100 Myr, and the duration of the quiescent phase is a few 10^5 to a few 10^8 yr (Konar et al. 2013b; Marecki & Szablewski 2009). As the outer relic lobes are expected to be steep spectral plasma, a few new DDRGs have been discovered using the low radio frequency observations with the GMRT: detailed spectral ageing analyses have been performed after incorporating complementary high-frequency data from the VLA (e.g., Saikia et al. 2006; Konar et al. 2006; Nandi et al. 2014). Tamhane et al. (2015) have discovered a new Mpc-sized radio galaxy at $z=1.32$ in the XMM-LSS field. This is a relic radio galaxy exhibiting co-spatial radio and X-ray lobe emission, but no core, jets or hotspots.

An important question in DDRGs is whether the jet power remains similar in two consecutive episodes. Konar & Hardcastle (2013) found strong evidence that the jet power, at least in a fraction of DDRGs, remains similar in two consecutive episodes: the injection spectral indices of inner and outer lobes were similar and an $\alpha_{inj}^{in} - \alpha_{inj}^{out}$ correlation between the injection spectral indices of inner and outer double, was detected. Konar & Hardcastle (2013) however, were studying only a few sources. With SKA, we expect to discover hundreds of DDRGs, so that one can verify the $\alpha_{inj}^{in} - \alpha_{inj}^{out}$ correlation and check for its universality. Konar & Hardcastle (2013) also found that the smallest duration of quiescent phase between two episodes (so far) was $\sim 10^5$ yr. A statistical study to find the distribution of quiescent phases of DDRGs is important to constrain the accretion physics of the central engine. With the expected discovery of many new DDRGs with SKA, we hope to study such a distribution.

Another important goal is to find the oldest plasma around the outer double of the known DDRGs. So far,

the oldest known plasma around a DDRG is 200 Myr in the source 4C 29.30 (Jamrozny et al. 2007). Since synchrotron ageing is a slow process at low electron energies, responsible for ~ 100 MHz radio emission, SKA will be able to detect radio relics that are as old as 100 million years. SKA is also likely to discover more triple-double radio galaxies. So far, there have only been three cases: B0925+420 (Brocksopp et al. 2007), Speca (Hota et al. 2011) and J1216+0709 (Singh et al. 2016). In the Seyfert galaxy Mrk 6, three episodes are seen in three different orientations (Kharb et al. 2006, see Figure 5). In NGC 5813, three pairs of cavities in X-ray emission have been found: these were later found to contain old relativistic plasma in GMRT observations (Randall et al. 2011). From the top left panel of Figure 1 of Prandoni & Seymour (2015), we see that the 5σ SKA *rms* noise at ~ 100 MHz is ~ 0.2 mJy beam⁻¹. This is much lower than most of the existing surveys, as well as *rms* noise of GMRT images ($1\sigma \sim$ a few mJy beam⁻¹) at 150 MHz after 8 hours of integration. The higher resolution of SKA will probe the jet-lobe structure well. This will be useful to discover new aspects of jet physics, as well as to verify the work discussed here.

Proctor (2011) and Machalski et al. (2001), have listed 242 systems including triple-double systems and over ~ 600 more candidates, in the VLA FIRST survey. Sirothia et al. (2009a) have listed 374 sources from an 18' square ELAIS-N1 field using the GMRT at 325 MHz up to a median *rms* noise of ~ 40 μ Jy and an angular resolution of $\sim 8''$. SKA1 surveys will be more sensitive than the GMRT ELAIS-N1. Extrapolating from these detections, and using Figure 1 from Johnston-Hollitt et al. (2015), we expect that the SKA surveys will detect $\sim 10^7$ DDRGs.

5.3. Episodic Activity in Low-luminosity AGN

Observations of the Seyfert galaxies NGC 4235 and NGC 4594 (the Sombrero galaxy), with the GMRT at 325 and 610 MHz, have revealed signatures of episodic AGN activity in them (Kharb et al. 2016). Both the 610 MHz total intensity and the 325 – 610 MHz spectral index images suggest the presence of a “relic” radio lobe in NGC 4235, suggestive of episodic activity in this galaxy. Based on a simple spectral ageing analysis, the relic outer lobe appears to be at least two times older than the present lobe. This implies that the AGN in NGC 4235 was switched “off” for the same time that it has been “on” for the current episode. A ~ 3 kpc linear, steep-spectrum “spur-like” feature is observed nearly perpendicular to the double-lobed structure in NGC 4594. Since the VLBI jet in NGC 4594 is perpendicular to this linear feature, the AGN does not seem to be currently fuelling it. The presence of this feature, detected in sensitive low frequency observations with the GMRT, therefore, also suggests episodic activity (see also Martini et al. 2003). The detection of diffuse low surface brightness emission from old and relic lobes, requires sensitive low frequency observations, as will become available with the SKA1-LOW survey at 120 MHz.

6. THE HIGH REDSHIFT UNIVERSE

It is important to discover high redshift radio galaxies for several reasons. Given the observed correlation between the steepness of the radio spectrum and cosmolog-

⁹ The Large Synoptic Survey Telescope

ical redshift (i.e., the $z - \alpha$ correlation), ultra steep spectrum (USS) radio sources are one of the efficient tracers of powerful HzRGs (Ishwara-Chandra et al. 2010a; Ker et al. 2012). Using deep 150 MHz ($1\sigma \sim 0.7$ mJy beam⁻¹) observations of LBDS-Lynx field, Ishwara-Chandra et al. (2010a) reported that among the 150 radio sources with spectra steeper than 1.0, about two-thirds of these are not detected in SDSS, and therefore suggested them to be strong HzRGs candidates. In contrast to searches for powerful HzRGs from radio surveys of moderate depths, fainter USS samples derived from deeper radio surveys can be useful in finding HzRGs at even higher redshifts and in unveiling a population of obscured weaker radio-loud AGN at moderate redshifts.

Using 325 MHz GMRT observations and 1.4 GHz VLA observations available in two subfields (VLA-VIMOS VLT Deep Survey, VLA-VVDS, and Subaru X-ray Deep Field, SXDF) of the XMM-LSS field, Singh et al. (2014) have derived a large sample of 160 faint USS radio sources and characterised their nature. Their study shows that the criterion of ultra steep spectral index remains a reasonably efficient method to select high- z sources even at sub-mJy flux densities. In addition to powerful HzRG candidates, their faint USS sample also contains populations of weaker radio-loud AGNs potentially hosted in obscured environments.

Using the $z - \alpha$ correlation, Ishwara-Chandra et al. (2011, 2010b) have found radio galaxies with $z > 3$ in the deep 150 MHz GMRT-LBDS-Lynx field images with an *rms* noise of ~ 0.7 mJy and an angular resolution of $\sim 17''$. Spectral indices were estimated by cross-correlating the data from these sources with the available data at 327, 610, 1400 and 4860 MHz from radio surveys like the Westerbork Northern Sky Survey and the VLA NVSS and FIRST. They detected about 765 sources in about 15 deg². 150 of these had spectra steeper than 1.0. Furthermore, about a 100 sources were not detected by SDSS, and are strong candidates for HzRGs. As the SKA1 survey will be higher in angular resolution and more sensitive than the GMRT at 150 MHz, we expect to detect a few million candidates for HzRGs in SKA level surveys (see Figure 1, Johnston-Hollitt et al. 2015).

6.1. Infrared-Faint Radio Sources

Recent deep radio surveys combined with auxiliary infrared surveys have discovered the population of Infrared-Faint Radio Sources (IFRS), that are relatively bright radio sources with faint or no counterparts in infrared and optical wavelengths (Middelberg et al. 2008; Norris et al. 2011). IFRS generally exhibit steep radio spectra ($\alpha > 1$), high brightness temperatures, $T_B \sim 10^6$ K, and polarisation in the radio, indicating them to be AGN rather than star forming galaxies (Norris et al. 2007; Banfield et al. 2011).

A search for 3.6 μ m counterparts of 1.4 GHz radio sources in 0.8 deg² of the SXDF, have yielded seven IFRS distributed over redshifts 1.7 to 4.2, with radio luminosities spanning over 10^{25} W Hz⁻¹ to 10^{27} W Hz⁻¹ (Singh et al. in preparation). This indicates that most, if not all, IFRS are potentially high-redshift ($z > 2$) radio-loud AGN suffering from heavy dust extinction. Zinn et al. (2011) have compiled a catalogue of 55 IFRS in four deep fields (CDFs ($S_{1.4\text{GHz}} \sim 186$ μ Jy at 5σ), ELAIS-S1

($S_{1.4\text{GHz}} \sim 160$ μ Jy at 5σ), FLS ($S_{1.4\text{GHz}} \sim 105$ μ Jy at 5σ), and COSMOS ($S_{1.4\text{GHz}} \sim 65$ μ Jy at 5σ)), although without redshift estimates. They have shown that the surface number density of IFRS increases with the depth of the radio survey, and can be best represented as $N_s = (30.8 \pm 15.0) \exp(-0.014 \pm 0.006) 5\sigma$, where N_s is the number of IFRS per deg², and σ is the *rms* noise in mJy beam⁻¹. Assuming the SKA1-survey 5σ flux density limit of 20 μ Jy beam⁻¹, the best fit equation gives an IFRS surface density of $\sim 30.8 \pm 15$. Therefore, we can expect to detect large number of IFRS using proposed SKA surveys. However, deep optical and IR observations will also be required to estimate their redshifts and to study their dusty host galaxies. Such data should become available from large area surveys like the LSST and VISTA¹⁰.

7. DUAL AGN IN GALAXY NUCLEI

In the merger driven picture of galaxy evolution, as galaxies merge, their supermassive black holes spiral into the centre of the merger remnant forming SMBH pairs (e.g., Begelman et al. 1980). If the black holes are accreting mass, they will form a binary or dual AGN. At separations of 1 to 10 kpc the accreting SMBH pairs are called dual AGN. At closer separations of a few times 10 parsec or less, the SMBH become gravitationally bound and form binary AGN. At this stage, stars are ejected from the surrounding region until finally the SMBH orbits shrink through the emission of gravitational radiation and the SMBH coalesce (Berczik et al. 2006). According to merger scenarios, dual AGN should be common in galaxies. However, the number of confirmed sub-kpc dual AGN is only around 20 (Deane et al. 2014; Müller-Sánchez et al. 2015). The low detection rate is partly because optical or X-ray observations cannot reach the required sub-arcsecond resolution, and partly due to dust obscuration. Radio observations are unaffected by dust obscuration and can yield sub-arcsecond images, making them the most efficient frequency for the detection of dual AGN.

Most of the early dual AGN were detected serendipitously due to radio variability (OJ 287; Valtonen et al. 2008), misaligned radio jets/lobes (e.g., RBS 797; Gitti et al. 2013) or double X-ray sources in galaxy nuclei (Fabiano et al. 2011). However, binary/dual AGN can be detected indirectly at optical wavelength using double peaked emission lines in the nuclear spectra of galaxies (e.g., Liu et al. 2010). The double peaks can arise from the Doppler shifts between the emission lines from the two AGN. Large samples of potential dual AGN have been drawn from the SDSS nuclear spectra of galaxies (Ge et al. 2012) using the [O III] emission line as the principal tracer, since it arises from the NLR in AGN. However, double peaked emission lines can also arise from bipolar outflows in AGN, super-winds from nuclear star formation or emission from gas rotating in accretion disks (Eracleous & Halpern 2003; Rosario et al. 2010; Kharb et al. 2015).

The SKA1-MID array using band 5 (frequency range 5 – 14 GHz) or SKA-VLBI, are needed to detect closely separated binary black holes. These configurations will result in angular resolutions ranging from 0.2 arcsec to

¹⁰ Visible and Infrared Survey Telescope for Astronomy

milli-arcseconds. Through high frequency 8 and 15 GHz observations with the EVLA, Khatun et al. (2016, in preparation) have detected the signatures of a precessing jet, likely arising from a binary black hole system, in a nearby double peaked emission line AGN. Dual or binary AGN at close separations are ideal candidates for gravitational wave studies of merging supermassive black holes. SKA will enable us to detect large samples of such candidates at radio frequencies, for targeted gravitational wave observations.

8. THE RADIO SKY AT μJy LEVELS

SKA will probe sub-mJy and μJy radio source population, which is believed to be largely associated with massive star forming galaxies. However, a significant fraction of the sub-mJy sources are also identified with low-luminosity AGN, with their fraction increasing with flux density (Garrett 2002). It is also likely that both starburst and AGN phenomena co-exist in many of the faint systems. The remaining fraction of the faint radio source population are associated with either extremely faint optical identifications, or remain unidentified altogether.

Deep radio observations of a few fields has led to the detection of many discrete radio sources in a single field of view (Garrett 2002). Several state-of-the-art modes of the SKA correlator, making full use of the raw data (e.g., mapping out the primary beam response of individual resolution elements in their entirety, or simultaneous multiple-field correlation) coupled with fast data output rates, would be key to achieving high angular resolution images of large areas of the sky in a single pointing. These radio images would then be matched to the large areas of the sky that are routinely being surveyed in great detail by optical and near-IR instruments. These studies will help us to disentangle the contributions of star-formation and AGN activity to radio emission in galaxies, and lead to the discovery of new types of radio-weak objects. In addition, the ‘tightness’ of the radio - FIR correlation will be tested to higher redshifts, where the correlation is expected to break down due to the dominance of inverse-Compton scattering (Schleicher & Beck 2013).

9. RADIO CONTINUUM SURVEYS WITH THE GMRT

The GMRT has been recognised as a pathfinder radio telescope for SKA. Here we briefly describe some of the deep and wide radio continuum surveys that have been carried out with the GMRT (see Table 3).

9.1. GMRT 325 MHz Survey of Herschel Fields

The XMM-LSS field has been surveyed with the GMRT at 325 MHz (Wadadekar et al. in preparation). This survey covers an area of $\sim 12 \text{ deg}^2$ and overlaps fully with the SWIRE and HerMES survey areas in the XMM-LSS field. The 325 MHz GMRT mosaic image has an average *rms* noise of $\sim 160 \mu\text{Jy beam}^{-1}$, while in the central region the *rms* noise reaches down to $\sim 120 \mu\text{Jy beam}^{-1}$, with a synthesized beam of $\sim 10''.2 \times 7''.9$. The 325 MHz survey of XMM-LSS is one of the deepest low-frequency surveys over such a wide sky area and it detects $\sim 2553/3304$ radio sources at $\geq 5\sigma$ with an *rms* noise cut-off $\leq 200/300 \mu\text{Jy beam}^{-1}$, where a

noise image is used for source extraction to account for non-uniformity. It is worth noting that these 325 MHz observations are about five times deeper than the previous 325 MHz observations of the XMM-LSS field (e.g., Cohen et al. 2003; Tasse et al. 2007), and result in a manifold increase in the source density.

Nearly 3.8 deg^2 area of the European Large-Area ISO Survey-North 1 (ELAIS-N1) field has been imaged at 325 MHz with the GMRT (Sirothia et al. 2009b). It is the most sensitive 325 MHz radio survey with a median *rms* noise of $\sim 40 \mu\text{Jy beam}^{-1}$: 1286 sources with a total flux density above $\sim 270 \mu\text{Jy}$ have been detected.

9.2. GMRT 610 MHz Survey

Garn et al. (2007) have carried out a 610 MHz survey of the Spitzer extragalactic First Look Survey field (xFLS). This survey covers a total area of $\sim 4 \text{ deg}^2$ in seven individual pointings with an *rms* noise of $\sim 30 \mu\text{Jy beam}^{-1}$ and resolution of $5''.8 \times 4''.7$. This survey has detected a total of 3944 sources above the 5σ level. The ELAIS-N1, Lockman Hole and VLA-VVDS have also been surveyed with the GMRT at 610 MHz (see Table 3).

9.3. 150 MHz GMRT Sky Survey

The TIFR GMRT Sky Survey (TGSS) is a radio continuum survey at 150 MHz carried out with GMRT. This survey covers $\sim 37,000 \text{ deg}^2$ of the sky north of declination of -53 degrees and reaches an *rms* noise level of $5-7 \text{ mJy beam}^{-1}$, with an angular resolution of $\sim 25''$ (Intema et al. 2016a). The first release TGSS has produced a catalog of 0.64 million radio sources at the 7σ level. More details about the TGSS can be found at <http://tgss.ncra.tifr.res.in/>. This survey and products from it will provide a reference for various new low-frequency telescopes, in particular SKA-LOW. Intema et al. (2011) carried out the 150 MHz GMRT survey of the NOVO Boötes field with an area coverage of $\sim 11.3 \text{ deg}^2$ and an *rms* noise of $\sim 1.0 \text{ mJy beam}^{-1}$.

10. NEW DIRECTIONS

In addition to expanding the scope of current AGN physics, there are exciting possibilities for new physics that will emerge from SKA. Given the order of magnitude increase in the sensitivity of the upcoming SKA surveys, we are likely to detect new classes of AGN. In particular, the radio-quiet or moderately radio-loud AGN hosted in dusty galaxies at high redshifts. In fact, the modelling of the X-ray background emission predicts a population of obscured AGN (Gilli et al. 2007), that has not so far been detected. We can also detect the first generation radio-loud AGN at redshifts > 7 (Afonso et al. 2015). These will place stringent constraints on the relationship between black hole masses, spins, accretion rates, and production of powerful jets, as the supermassive black holes would have formed around then, in the hierarchical galaxy evolution model (e.g., Li et al. 2007).

Furthermore, radio AGN that are now considered outliers, like hybrid FRI/II sources, X-shaped or highly distorted jet sources, or ‘‘intermediate’’ sources that lie close to the radio-loud/radio-quiet divide, or several times restarted AGN sources, could turn out to be norm when observing the radio Universe at high sensitivity. With the detection of many more such sources, it will become

possible to create their luminosity functions, and examine their evolution and redshift distributions. Questions of the kind, ‘are sources at the *cusp* transitioning from one AGN class to another?’, will be answered. For instance, it has been hypothesised that FRII radio galaxies evolve into FRI radio galaxies (e.g., Baum et al. 1995). Are hybrid FRI/II sources then the transitioning objects? This can be rigorously tested when more hybrid and FRI sources with weak diffuse lobes are discovered at higher redshifts. These discoveries are expected to fundamentally alter our view of AGN, of galaxies, and of the Universe.

11. CONCLUDING REMARKS

We have summarised various science interests of a large fraction of the AGN community in India. Whether it comes to detecting “intermediate” sources between the radio-loud and radio-quiet classes, or “intermediate” sources between FRIs and FRIIs, relic emission from previous activities of the AGN, giant radio jets in spiral galaxies, double-double or triple-double radio galaxies, or faint ultra-steep spectrum sources at high redshifts, higher sensitivity data that are at present unavailable, are required. The various SKA configurations and the upcoming SKA surveys will meet these needs. VLBI is required to probe the regions close to the central black holes. Again, an increase in sensitivity is crucial. SKA-VLBI which could include large single antennas like the upcoming FAST radio telescope, will be able to study parsec and sub-parsec-scale radio jets and their magnetic field structures in low luminosity AGN, which have so far remained below the sensitivity limits of the current VLBI arrays. In short, several burning questions on AGN physics, the answers to which have primarily been limited by the lack of resolution, sensitivity or statistically significant number of sources, will be addressed directly by SKA. Many more new leading questions on AGN physics will hopefully be raised.

We thank the anonymous referee for their careful reading of our manuscript and providing insightful suggestions that have improved this paper. MP is thankful to the CEFIPRA organization for the Franco-Indian research grant.

REFERENCES

- Afonso, J., Casanellas, J., Prandoni, I., Jarvis, M., Lorenzoni, S., Magliocchetti, M., & Seymour, N. 2015, *Advancing Astrophysics with the Square Kilometre Array (AASKA14)*, 71
- Antonucci, R. 1993, *ARA&A*, 31, 473
- Bagchi, J., Vivek, M., Vikram, V., Hota, A., Biju, K. G., Sirothia, S. K., Srikanand, R., Gopal-Krishna, & Jacob, J. 2014, *ApJ*, 788, 174
- Banfield, J. K., George, S. J., Taylor, A. R., Stil, J. M., Kothes, R., & Scott, D. 2011, *ApJ*, 733, 69
- Barnes, J. E., & Hernquist, L. 1992, *ARA&A*, 30, 705
- Baum, S. A., Zirbel, E. L., & O’Dea, C. P. 1995, *ApJ*, 451, 88
- Becker, R. H., White, R. L., & Helfand, D. J. 1995, *ApJ*, 450, 559
- Beckwith, K., Hawley, J. F., & Krolik, J. H. 2008, *ApJ*, 678, 1180
- Begelman, M. C., Blandford, R. D., & Rees, M. J. 1980, *Nature*, 287, 307
- Berczik, P., Merritt, D., Spurzem, R., & Bischof, H.-P. 2006, *ApJL*, 642, L21
- Best, P. N., & Heckman, T. M. 2012, *MNRAS*, 421, 1569
- Bicknell, G. V. 1986, *ApJ*, 300, 591
- Blandford, R. D. 1993, *Astrophysical Jets (Space Telescope Science Inst. Symp. Ser.6, eds. D. Burgarella, M. Livio, & C. P. O’Dea (Cambridge Univ. Press), p.15)*
- Blandford, R. D., & Payne, D. G. 1982, *MNRAS*, 199, 883
- Blandford, R. D., & Znajek, R. L. 1977, *MNRAS*, 179, 433
- Bondi, M., Ciliegi, P., Venturi, T., Dallacasa, D., Bardelli, S., Zucca, E., Athreya, R. M., Gregorini, L., Zanichelli, A., Le Fèvre, O., Contini, T., Garilli, B., Iovino, A., Tempurin, S., & Vergani, D. 2007, *A&A*, 463, 519
- Brocksopp, C., Kaiser, C. R., Schoenmakers, A. P., & de Bruyn, A. G. 2007, *MNRAS*, 382, 1019
- Chandra, S., Baliyan, K. S., Ganesh, S., & Foschini, L. 2014, *ApJ*, 791, 85
- Chandra, S., Baliyan, K. S., Ganesh, S., & Joshi, U. C. 2012, *ApJ*, 746, 92
- Cheung, C. C. 2007, *AJ*, 133, 2097
- Cohen, A. S., Röttgering, H. J. A., Kassim, N. E., Cotton, W. D., Perley, R. A., Wilman, R., Best, P., Pierre, M., Birkinshaw, M., Bremer, M., & Zanichelli, A. 2003, *ApJ*, 591, 640
- Comerford, J. M., Schluns, K., Greene, J. E., & Cool, R. J. 2013, *ApJ*, 777, 64
- Condon, J. J., Cotton, W. D., Greisen, E. W., Yin, Q. F., Perley, R. A., Taylor, G. B., & Broderick, J. J. 1998, *AJ*, 115, 1693
- Cox, T. J., Jonsson, P., Primack, J. R., & Somerville, R. S. 2006, *MNRAS*, 373, 1013
- Croton, D. J., Springel, V., White, S. D. M., De Lucia, G., Frenk, C. S., Gao, L., Jenkins, A., Kauffmann, G., Navarro, J. F., & Yoshida, N. 2006, *MNRAS*, 365, 11
- Davé, R., Cen, R., Ostriker, J. P., Bryan, G. L., Hernquist, L., Katz, N., Weinberg, D. H., Norman, M. L., & O’Shea, B. 2001, *ApJ*, 552, 473
- Davies, R. D. 1990, in *New Windows to the Universe*, ed. F. Sanchez & M. Vazquez, Vol. 2, 81–99
- Deane, R. P., Paragi, Z., Jarvis, M. J., Coriat, M., Bernardi, G., Fender, R. P., Frey, S., Heywood, I., Klöckner, H.-R., Grainge, K., & Rumsey, C. 2014, *Nature*, 511, 57
- Dewdney, P., Turner, W., Millenaar, R., McCool, R., Lazio, J., & Cornwell, T. 2013, “SKA1 System Baseline Design”, Document number SKA-TEL-SKO-DD-001 Revision 1
- Eracleous, M., & Halpern, J. P. 2003, *ApJ*, 599, 886
- Fabbiano, G., Wang, J., Elvis, M., & Risaliti, G. 2011, *Nature*, 477, 431
- Fanaroff, B. L., & Riley, J. M. 1974, *MNRAS*, 167, 31P
- Fossati, G., Maraschi, L., Celotti, A., Comastri, A., & Ghisellini, G. 1998, *MNRAS*, 299, 433
- Gabuzda, D. C., Knuettel, S., & Bonafede, A. 2015, *A&A*, 583, A96
- Gabuzda, D. C., Mullan, C. M., Cawthorne, T. V., Wardle, J. F. C., & Roberts, D. H. 1994, *ApJ*, 435, 140
- Gabuzda, D. C., Reichstein, A. R., & O’Neill, E. L. 2014, *MNRAS*, 444, 172
- Galametz, A., Stern, D., De Breuck, C., Hatch, N., Mayo, J., Miley, G., Rettura, A., Seymour, N., Stanford, S. A., & Vernet, J. 2012, *ApJ*, 749, 169
- Gallimore, J. F., Axon, D. J., O’Dea, C. P., Baum, S. A., & Pedlar, A. 2006, *AJ*, 132, 546
- Garn, T., Green, D. A., Hales, S. E. G., Riley, J. M., & Alexander, P. 2007, *MNRAS*, 376, 1251
- Garn, T., Green, D. A., Riley, J. M., & Alexander, P. 2008, *MNRAS*, 383, 75
- Garn, T. S., Green, D. A., Riley, J. M., & Alexander, P. 2010, *Bulletin of the Astronomical Society of India*, 38, 103
- Garofalo, D. 2013, *MNRAS*, 434, 3196
- Garrett, M. A. 2002, *A&A*, 384, L19
- Ge, J.-Q., Hu, C., Wang, J.-M., Bai, J.-M., & Zhang, S. 2012, *ApJS*, 201, 31
- Gilli, R., Comastri, A., & Hasinger, G. 2007, *A&A*, 463, 79
- Gitti, M., Giroletti, M., Giovannini, G., Feretti, L., & Liuzzo, E. 2013, *A&A*, 557, L14
- Greene, J. E., & Ho, L. C. 2007, *ApJ*, 667, 131
- Hardcastle, M. J., Evans, D. A., & Croston, J. H. 2007, *MNRAS*, 376, 1849
- Harris, D. E., & Krawczynski, H. 2006, *ARA&A*, 44, 463
- Heckman, T. M., Smith, E. P., Baum, S. A., van Breugel, W. J. M., Miley, G. K., Illingworth, G. D., Bothun, G. D., & Balick, B. 1986, *ApJ*, 311, 526

- Ho, L., & Kormendy, J. 2000, *Supermassive Black Holes in Active Galactic Nuclei*, ed. P. Murdin
- Ho, L. C., & Peng, C. Y. 2001, *ApJ*, 555, 650
- Hota, A., Croston, J. H., Ohya, Y., Stalin, C. S., Hardcastle, M. J., Konar, C., Aravind, R. P., Agarwal, S. M., Dharmik Bhoga, S. A., Dabhade, P. A., Kamble, A. A., Mohanty, P. K., Mukherjee, A., Pandey, A. V., Patra, A., Pechetti, R., Raut, S. S., Sushma, V., Vaddi, S., & Verma, N. 2014, *ArXiv e-prints*
- Hota, A., Sirothia, S. K., Ohya, Y., Konar, C., Kim, S., Rey, S.-C., Saikia, D. J., Croston, J. H., & Matsushita, S. 2011, *MNRAS*, 417, L36
- Hovatta, T., Lister, M. L., Aller, M. F., Aller, H. D., Homan, D. C., Kovalev, Y. Y., Pushkarev, A. B., & Savolainen, T. 2012, *AJ*, 144, 105
- Ibar, E., Ivison, R. J., Biggs, A. D., Lal, D. V., Best, P. N., & Green, D. A. 2009, *MNRAS*, 397, 281
- Intema, H. T., Jagannathan, P., Mooley, K. P., & Frail, D. A. 2016a, *ArXiv e-prints*
- 2016b, *ArXiv e-prints*
- Intema, H. T., van Weeren, R. J., Röttgering, H. J. A., & Lal, D. V. 2011, *A&A*, 535, A38
- Ishwara-Chandra, C. H., & Saikia, D. J. 1999, *MNRAS*, 309, 100
- Ishwara-Chandra, C. H., Sirothia, S. K., Wadadekar, Y., & Pal, S. 2011, *Journal of Astrophysics and Astronomy*, 32, 609
- Ishwara-Chandra, C. H., Sirothia, S. K., Wadadekar, Y., Pal, S., & Windhorst, R. 2010a, *MNRAS*, 405, 436
- 2010b, *MNRAS*, 405, 436
- Jamrozy, M., Konar, C., Saikia, D. J., Stawarz, L., Mack, K.-H., & Siemiginowska, A. 2007, *MNRAS*, 378, 581
- Jamrozy, M., Saikia, D. J., & Konar, C. 2009, *MNRAS*, 399, L141
- Johnston-Hollitt, M., Dehghan, S., & Pratley, L. 2015, *Advancing Astrophysics with the Square Kilometre Array (AASKA14)*, 101
- Kellermann, K. I., Sramek, R., Schmidt, M., Shaffer, D. B., & Green, R. 1989, *AJ*, 98, 1195
- Ker, L. M., Best, P. N., Rigby, E. E., Röttgering, H. J. A., & Gendre, M. A. 2012, *MNRAS*, 420, 2644
- Kharb, P., Das, M., Paragi, Z., Subramanian, S., & Chitta, L. P. 2015, *ApJ*, 799, 161
- Kharb, P., Gabuzda, D. C., O’Dea, C. P., Shastri, P., & Baum, S. A. 2009, *ApJ*, 694, 1485
- Kharb, P., Lister, M. L., & Cooper, N. J. 2010, *ApJ*, 710, 764
- Kharb, P., O’Dea, C. P., Baum, S. A., Colbert, E. J. M., & Xu, C. 2006, *ApJ*, 652, 177
- Kharb, P., O’Dea, C. P., Baum, S. A., Daly, R. A., Mory, M. P., Donahue, M., & Guerra, E. J. 2008, *ApJS*, 174, 74
- Kharb, P., O’Dea, C. P., Baum, S. A., Hardcastle, M. J., Dicken, D., Croston, J. H., Mingo, B., & Noel-Storr, J. 2014, *MNRAS*, 440, 2976
- Kharb, P., O’Dea, C. P., Tilak, A., Baum, S. A., Haynes, E., Noel-Storr, J., Fallon, C., & Christiansen, K. 2012, *ApJ*, 754, 1
- Kharb, P., Shastri, P., & Gabuzda, D. C. 2005, *ApJL*, 632, L69
- Kharb, P., Srivastava, S., Singh, V., Gallimore, J. F., Ishwara-Chandra, C. H., & Ananda, H. 2016, *MNRAS*, 459, 1310
- Konar, C., & Hardcastle, M. J. 2013, *MNRAS*, 436, 1595
- Konar, C., Hardcastle, M. J., Jamrozy, M., & Croston, J. H. 2013a, *MNRAS*, 430, 2137
- 2013b, *MNRAS*, 430, 2137
- Konar, C., Saikia, D. J., Jamrozy, M., & Machalski, J. 2006, *MNRAS*, 372, 693
- Kormendy, J., & Ho, L. C. 2013, *ARA&A*, 51, 511
- Laing, R. A. 1993, in *Sub-arcsecond Radio Astronomy*, ed. R. J. Davis & R. S. Booth, 346
- Laing, R. A. 1996, in *IAU Symposium, Vol. 175, Extragalactic Radio Sources*, ed. R. D. Ekers, C. Fanti, & L. Padrielli, 147
- Laing, R. A., & Bridle, A. H. 2002, *MNRAS*, 336, 1161
- Lal, D. V., & Ho, L. C. 2010, *AJ*, 139, 1089
- Lal, D. V., Kraft, R. P., Forman, W. R., Hardcastle, M. J., Jones, C., Nulsen, P. E. J., Evans, D. A., Croston, J. H., & Lee, J. C. 2010, *ApJ*, 722, 1735
- Lal, D. V., Kraft, R. P., Randall, S. W., Forman, W. R., Nulsen, P. E. J., Roediger, E., Zuhone, J. A., Hardcastle, M. J., Jones, C., & Croston, J. H. 2013, *ApJ*, 764, 83
- Lal, D. V., & Rao, A. P. 2005, *MNRAS*, 356, 232
- 2007, *MNRAS*, 374, 1085
- Lal, D. V., Shastri, P., & Gabuzda, D. C. 2004, *A&A*, 425, 99
- 2011, *ApJ*, 731, 68
- Landt, H., Perlman, E. S., & Padovani, P. 2006, *ApJ*, 637, 183
- Laor, A. 2000, *ApJL*, 543, L111
- Ledlow, M. J., & Owen, F. N. 1996, *AJ*, 112, 9
- Ledlow, M. J., Owen, F. N., & Keel, W. C. 1998, *ApJ*, 495, 227
- Li, Y., Hernquist, L., Robertson, B., Cox, T. J., Hopkins, P. F., Springel, V., Gao, L., Di Matteo, T., Zentner, A. R., Jenkins, A., & Yoshida, N. 2007, *ApJ*, 665, 187
- Lister, M. L., Cohen, M. H., Homan, D. C., Kadler, M., Kellermann, K. I., Kovalev, Y. Y., Ros, E., Savolainen, T., & Zensus, J. A. 2009, *AJ*, 138, 1874
- Liu, R., & Pooley, G. 1991, *MNRAS*, 253, 669
- Liu, X., Greene, J. E., Shen, Y., & Strauss, M. A. 2010, *ApJL*, 715, L30
- Lynden-Bell, D. 1969, *Nature*, 223, 690
- Machalski, J., Jamrozy, M., & Zola, S. 2001, *A&A*, 371, 445
- Malarecki, J. M., Staveley-Smith, L., Saripalli, L., Subrahmanyam, R., Jones, D. H., Duffy, A. R., & Rioja, M. 2013, *MNRAS*, 432, 200
- Mao, M. Y., Owen, F., Duffin, R., Keel, B., Lacy, M., Momjian, E., Morrison, G., Mroczkowski, T., Neff, S., Norris, R. P., Schmitt, H., Toy, V., & Veilleux, S. 2015, *MNRAS*, 446, 4176
- Marecki, A., & Szablewski, M. 2009, *A&A*, 506, L33
- Martini, P., Regan, M. W., Mulchaey, J. S., & Pogge, R. W. 2003, *ApJ*, 589, 774
- Mauch, T., Klöckner, H.-R., Rawlings, S., Jarvis, M., Hardcastle, M. J., Obreschkow, D., Saikia, D. J., & Thompson, M. A. 2013, *MNRAS*, 435, 650
- McKinney, J. C. 2006, *MNRAS*, 368, 1561
- McLure, R. J., Kukula, M. J., Dunlop, J. S., Baum, S. A., O’Dea, C. P., & Hughes, D. H. 1999, *MNRAS*, 308, 377
- McLure, R. J., Willott, C. J., Jarvis, M. J., Rawlings, S., Hill, G. J., Mitchell, E., Dunlop, J. S., & Wold, M. 2004, *MNRAS*, 351, 347
- Meier, D. L. 1999, *ApJ*, 522, 753
- Merloni, A., Heinz, S., & di Matteo, T. 2003, *MNRAS*, 345, 1057
- Middelberg, E., Norris, R. P., Tingay, S., Mao, M. Y., Phillips, C. J., & Hotan, A. W. 2008, *A&A*, 491, 435
- Mihos, J. C., & Hernquist, L. 1996, *ApJ*, 464, 641
- Müller-Sánchez, F., Comerford, J. M., Nevin, R., Barrows, R. S., Cooper, M. C., & Greene, J. E. 2015, *ApJ*, 813, 103
- Nan, R., Li, D., Jin, C., Wang, Q., Zhu, L., Zhu, W., Zhang, H., Yue, Y., & Qian, L. 2011, *International Journal of Modern Physics D*, 20, 989
- Nandi, S., Roy, R., Saikia, D. J., Singh, M., Chandola, H. C., Baes, M., Joshi, R., Gentile, G., & Patgiri, M. 2014, *ApJ*, 789, 16
- Nandi, S., & Saikia, D. J. 2012, *Bulletin of the Astronomical Society of India*, 40, 121
- Nath, B. B. 1995, *MNRAS*, 274, 208
- 2010, *MNRAS*, 407, 1998
- Netzer, H. 2015, *ARA&A*, 53, 365
- Norris, R. P., Afonso, J., Cava, A., Farrah, D., Huynh, M. T., Ivison, R. J., Jarvis, M., Lacy, M., Mao, M., Maraston, C., Mauduit, J.-C., Middelberg, E., Oliver, S., Seymour, N., & Surace, J. 2011, *ApJ*, 736, 55
- Norris, R. P., Tingay, S., Phillips, C., Middelberg, E., Deller, A., & Appleton, P. N. 2007, *MNRAS*, 378, 1434
- O’Dea, C. P., & Owen, F. N. 1985, *AJ*, 90, 927
- Padovani, P., & Giommi, P. 1995, *MNRAS*, 277, 1477
- Pandey-Pommier, M., Sirothia, S., Chadwick, P., Martin, J.-M., Colom, P., van Driel, W., Combes, F., Kharb, P., Crespeau, P., Richard, J., & Guiderdoni, B. 2016, *ArXiv e-prints* (1610.05650)
- Paragi, Z., Godfrey, L., Reynolds, C., & 79 coauthors. 2015, *Advancing Astrophysics with the Square Kilometre Array (AASKA14)*, 143
- Pedley, J. A., Rudnick, L., McCarthy, P. J., & Spinrad, H. 1989, *AJ*, 97, 647
- Prandoni, I., & Seymour, N. 2015, *Advancing Astrophysics with the Square Kilometre Array (AASKA14)*, 67
- Prestage, R. M., & Peacock, J. A. 1988, *MNRAS*, 230, 131
- Proctor, D. D. 2011, *ApJS*, 194, 31
- Punsly, B., Marziani, P., Kharb, P., O’Dea, C. P., & Vestergaard, M. 2015, *ApJ*, 812, 79

- Randall, S. W., Forman, W. R., Giacintucci, S., Nulsen, P. E. J., Sun, M., Jones, C., Churazov, E., David, L. P., Kraft, R., Donahue, M., Blanton, E. L., Simionescu, A., & Werner, N. 2011, *ApJ*, 726, 86
- Rees, M. J., Begelman, M. C., Blandford, R. D., & Phinney, E. S. 1982, *Nature*, 295, 17
- Reichstein, A., & Gabuzda, D. 2010, in *Astronomical Society of the Pacific Conference Series*, Vol. 427, *Accretion and Ejection in AGN: a Global View*, ed. L. Maraschi, G. Ghisellini, R. Della Ceca, & F. Tavecchio, 211
- Rodriguez, C., Taylor, G. B., Zavala, R. T., Peck, A. B., Pollack, L. K., & Romani, R. W. 2006, *ApJ*, 646, 49
- Rosario, D. J., McGurk, R. C., Max, C. E., Shields, G. A., Smith, K. L., & Ammons, S. M. 2011, *ApJ*, 739, 44
- Rosario, D. J., Shields, G. A., Taylor, G. B., Salviander, S., & Smith, K. L. 2010, *ApJ*, 716, 131
- Saikia, D. J., & Jamrozy, M. 2009, *Bulletin of the Astronomical Society of India*, 37
- Saikia, D. J., Konar, C., & Kulkarni, V. K. 2006, *MNRAS*, 366, 1391
- Sambruna, R. M., Maraschi, L., & Urry, C. M. 1996, *ApJ*, 463, 444
- Schleicher, D. R. G., & Beck, R. 2013, *A&A*, 556, A142
- Schoenmakers, A. P., de Bruyn, A. G., Röttgering, H. J. A., van der Laan, H., & Kaiser, C. R. 2000, *MNRAS*, 315, 371
- Schweizer, F. 1982, *ApJ*, 252, 455
- 1986, *Science*, 231, 227
- Seymour, N., Stern, D., De Breuck, C., Vernet, J., Rettura, A., Dickinson, M., Dey, A., Eisenhardt, P., Fosbury, R., Lacy, M., McCarthy, P., Miley, G., Rocca-Volmerange, B., Röttgering, H., Stanford, S. A., Teplitz, H., van Breugel, W., & Zirm, A. 2007, *ApJS*, 171, 353
- Sikora, M., & Begelman, M. C. 2013, *ApJL*, 764, L24
- Sikora, M., Stawarz, L., & Lasota, J.-P. 2007, *ApJ*, 658, 815
- Singh, V., Beelen, A., Wadadekar, Y., Sirothia, S., Ishwara-Chandra, C. H., Basu, A., Omont, A., McAlpine, K., Ivison, R. J., Oliver, S., Farrah, D., & Lacy, M. 2014, *A&A*, 569, A52
- Singh, V., Ishwara-Chandra, C. H., Kharb, P., Srivastava, S., & Janardhan, P. 2016, *ApJ*, 826, 132
- Singh, V., Ishwara-Chandra, C. H., Sievers, J., Wadadekar, Y., Hilton, M., & Beelen, A. 2015a, *MNRAS*, 454, 1556
- Singh, V., Ishwara-Chandra, C. H., Wadadekar, Y., Beelen, A., & Kharb, P. 2015b, *MNRAS*, 446, 599
- Sirothia, S. K., Dennefeld, M., Saikia, D. J., Dole, H., Ricquebourg, F., & Roland, J. 2009a, *MNRAS*, 395, 269
- 2009b, *MNRAS*, 395, 269
- Sparks, W. B., Baum, S. A., Biretta, J., Macchetto, F. D., & Martel, A. R. 2000, *ApJ*, 542, 667
- Stanley, E. C., Kharb, P., Lister, M. L., Marshall, H. L., O’Dea, C., & Baum, S. 2015, *ApJ*, 807, 48
- Tamhane, P., Wadadekar, Y., Basu, A., Singh, V., Ishwara-Chandra, C. H., Beelen, A., & Sirothia, S. 2015, *MNRAS*, 453, 2438
- Tasse, C., Röttgering, H. J. A., Best, P. N., Cohen, A. S., Pierre, M., & Wilman, R. 2007, *A&A*, 471, 1105
- Taylor, A. R., & Jagannathan, P. 2016, *MNRAS*, 459, L36
- Tchekhovskoy, A., Narayan, R., & McKinney, J. C. 2010, *ApJ*, 711, 50
- 2011, *MNRAS*, 418, L79
- Ulvestad, J. S., Wrobel, J. M., Roy, A. L., Wilson, A. S., Falcke, H., & Krichbaum, T. P. 1999, *ApJL*, 517, L81
- Urry, C. M., & Padovani, P. 1995, *PASP*, 107, 803
- Valtonen, M. J., Lehto, H. J., Nilsson, K., Heidt, J., Takalo, L. O., Sillanpää, A., Villforth, C., Kidger, M., Poyner, G., Pursimo, T., Zola, S., Wu, J.-H., Zhou, X., Sadakane, K., Drozd, M., Koziel, D., Marchev, D., Ogloza, W., Porowski, C., Siwak, M., Stachowski, G., Winiarski, M., Hentunen, V.-P., Nissinen, M., Liakos, A., & Dogru, S. 2008, *Nature*, 452, 851
- Venemans, B. P., Röttgering, H. J. A., Miley, G. K., van Breugel, W. J. M., de Breuck, C., Kurk, J. D., Pentericci, L., Stanford, S. A., Overzier, R. A., Croft, S., & Ford, H. 2007, *A&A*, 461, 823
- Werner, N., Finoguenov, A., Kaastra, J. S., Simionescu, A., Dietrich, J. P., Vink, J., & Böhringer, H. 2008, *A&A*, 482, L29
- Worrall, D. M., Birkinshaw, M., & Hardcastle, M. J. 2001, *MNRAS*, 326, L7
- York, D. G., Adelman, J., Anderson, Jr., J. E., Anderson, S. F., Annis, J., Bahcall, N. A., Bakken, J. A., Barkhouser, R., Bastian, S., Berman, E., Boroski, W. N., Bracker, S., Briegel, C., Briggs, J. W., Brinkmann, J., Brunner, R., Burles, S., Carey, L., Carr, M. A., Castander, F. J., Chen, B., Colestock, P. L., Connolly, A. J., Crocker, J. H., Csabai, I., Czarapata, P. C., Davis, J. E., Doi, M., Dombek, T., Eisenstein, D., Ellman, N., Elms, B. R., Evans, M. L., Fan, X., Federwitz, G. R., Fiscelli, L., Friedman, S., Frieman, J. A., Fukugita, M., Gillespie, B., Gunn, J. E., Gurbani, V. K., de Haas, E., Haldeman, M., Harris, F. H., Hayes, J., Heckman, T. M., Hennessy, G. S., Hindsley, R. B., Holm, S., Holmgren, D. J., Huang, C.-h., Hull, C., Husby, D., Ichikawa, S.-I., Ichikawa, T., Ivezić, Z., Kent, S., Kim, R. S. J., Kinney, E., Klaene, M., Kleinman, A. N., Kleinman, S., Knapp, G. R., Korienek, J., Kron, R. G., Kunszt, P. Z., Lamb, D. Q., Lee, B., Leger, R. F., Limmongkol, S., Lindenmeyer, C., Long, D. C., Loomis, C., Loveday, J., Lucinio, R., Lupton, R. H., MacKinnon, B., Mannery, E. J., Mantsch, P. M., Margon, B., McGehee, P., McKay, T. A., Meiksin, A., Merelli, A., Monet, D. G., Munn, J. A., Narayanan, V. K., Nash, T., Neilsen, E., Neswold, R., Newberg, H. J., Nichol, R. C., Nicinski, T., Nonino, M., Okada, N., Okamura, S., Ostriker, J. P., Owen, R., Pauls, A. G., Peoples, J., Peterson, R. L., Petravick, D., Pier, J. R., Pope, A., Pordes, R., Prosapio, A., Rechenmacher, R., Quinn, T. R., Richards, G. T., Richmond, M. W., Rivetta, C. H., Rockosi, C. M., Ruthmansdorfer, K., Sandford, D., Schlegel, D. J., Schneider, D. P., Sekiguchi, M., Sergey, G., Shimasaku, K., Siegmund, W. A., Smee, S., Smith, J. A., Snedden, S., Stone, R., Stoughton, C., Strauss, M. A., Stubbs, C., SubbaRao, M., Szalay, A. S., Szapudi, I., Szokoly, G. P., Thakar, A. R., Tremonti, C., Tucker, D. L., Uomoto, A., Vanden Berk, D., Vogeley, M. S., Waddell, P., Wang, S.-i., Watanabe, M., Weinberg, D. H., Yanny, B., Yasuda, N., & SDSS Collaboration. 2000, *AJ*, 120, 1579
- Zinn, P.-C., Middelberg, E., & Ibar, E. 2011, *A&A*, 531, A14

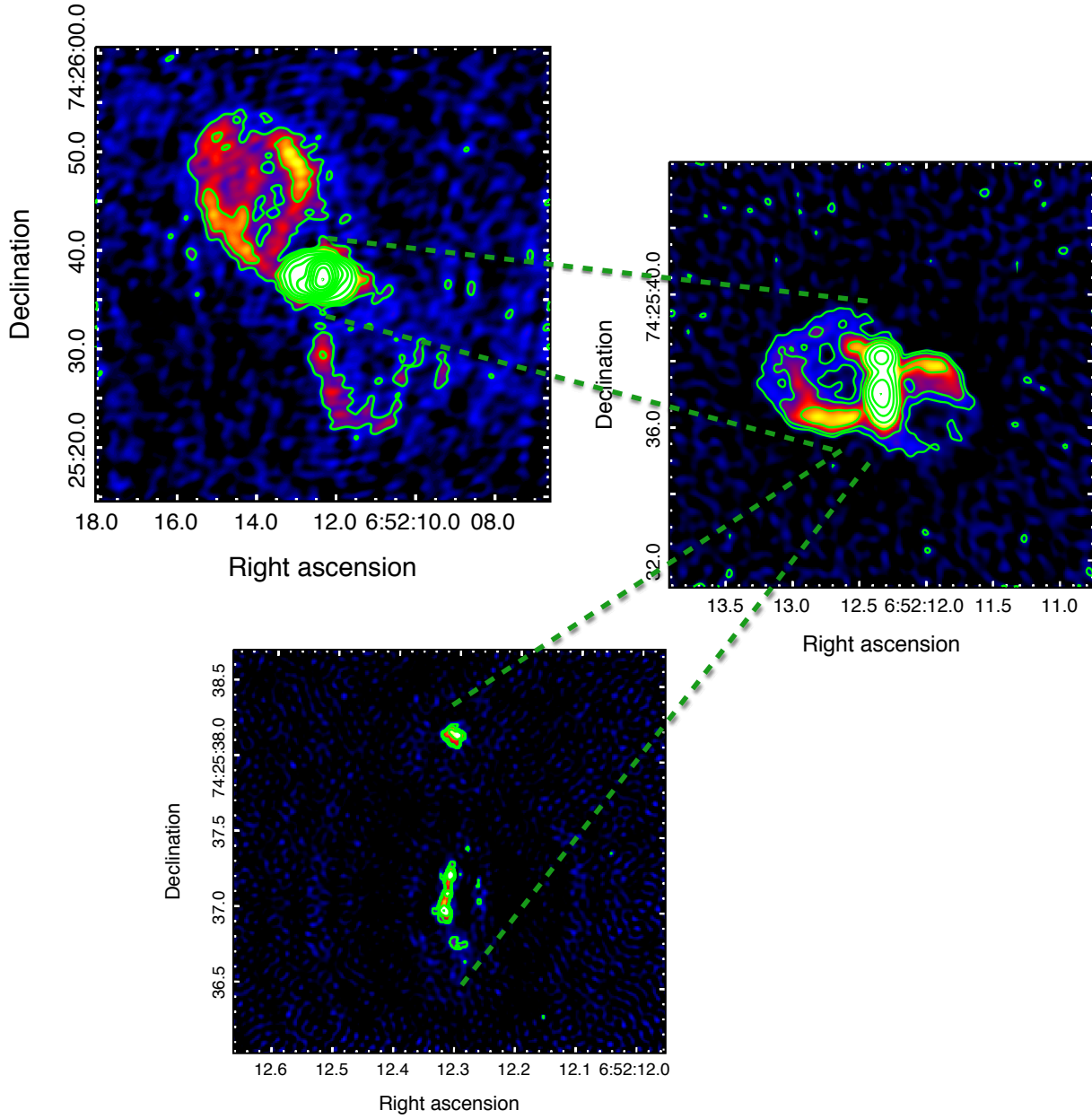


Figure 5. The Seyfert galaxy Markarian 6 exhibits three sets of radio lobes/jets which are nearly perpendicular to each other (Kharb et al. 2006). The detection of these structures required sensitive observations with multiple arrays and frequencies with the VLA and MERLIN. Steep-spectrum radio lobes from previous episodes of the AGN activity require sensitive low frequency observations, as will become available with SKA. Many such complex radio morphology sources are likely to be detected then.

Table 3
GMRT radio continuum surveys of extragalactic fields

Frequency (MHz)	Field	Area (deg ²)	<i>rms</i> noise (mJy beam ⁻¹)	beam-size	Reference
610	Lockman Hole	0.2	0.015	7".1 × 6".5	Ibar et al. (2009)
610	VLA-VVDS	1.0	0.05	6".0 × 5".0	Bondi et al. (2007)
610	xFLS	4.0	0.03	5".8 × 4".7	Garn et al. (2007)
610	Lockman Hole	8.0	0.08	6".0 × 5".0	Garn et al. (2010)
610	ELAIS-N1	9.0	0.04 – 0.07	6".0 × 5".0	Garn et al. (2008)
610	ELAIS-N1	1.0	0.01	6".0 × 5".0	Taylor & Jagannathan (2016)
325	ELAIS-N1	1.1	0.04	9".4 × 7".4	Sirothia et al. (2009b)
325	XMM-LSS	12	0.15	10".2 × 7".9	Wadadekar et al. in preparation
325	H-ATLAS	90	1.0	14" – 24"	Mauch et al. (2013)
150	NOVO Boötes	11.3	1.0	26" × 22"	Intema et al. (2011)
150	TGSS	36900	3.5	25" × 25"	Intema et al. (2016b)